Y. Fu, W. Zuo, M. Wetter, J. W. VanGilder, X. Han, D. Plamondon 2019. "Equation-Based Object-Oriented Modeling and Simulation for Data Center Cooling: A Case Study." Energy and Buildings, 186, pp. 108-125. DOI: 10.1016/j.enbuild.2019.01.018

Equation-Based Object-Oriented Modeling and Simulation for Data Center Cooling: A Case Study

Yangyang Fu[a], Wangda Zuo[a,*], Michael Wetter[b], Jim W. VanGilder[c], Xu Han[a], David Plamondon[d]

[a] Department of Civil, Architectural and Environmental Engineering, University of Colorado at Boulder, Boulder, CO, 80309, USA

[b] Building Technology and Urban Systems, Lawrence Berkeley National Laboratory, Berkeley, CA, 94720, USA

[c] Schneider Electric, Andover, MA, 01810, USA

[d] University of Massachusetts Medical School, Worcester, MA, 01655, USA

* Corresponding Author: wangda.zuo@colorado.edu

Abstract

Data center cooling accounts for about 1% of electricity usage in the United States. Computer models are pivotal in designing and operating energy-efficient cooling systems. Compared to conventional building performance simulation programs, the equation-based object-oriented modeling language Modelica is an emerging approach that can enable fast prototyping and dynamic simulation of cooling systems. In this case study, we first modeled the cooling and control systems of an actual data center located in Massachusetts using the open-source Modelica Buildings library, and then calibrated a baseline model based on measurement data. The simulation of the baseline model identified several operation-related issues in the cooling and control systems, such as degraded cooling coils, improper dead band in control settings, and simultaneous cooling and heating in air handlers. Afterwards, we used a sequential search technique as well as an optimization scheme to investigate the energy saving potentials for different energy efficiency measures aiming to address the abovementioned issues. Simulation results show potential energy savings up to 24% by resolving identified control-related issues and optimizing the supply air temperature.

Keywords: Equation-Based, Object-Oriented, Modelica, Data Center

1 Introduction

Data centers are critical, energy-intensive infrastructure that support the fast growth of the information technology (IT) industry and the transformation of the economy at large [1]. In 2010 data centers consumed about 1.1% to 1.5% of the total worldwide electricity and about 1.7% to

2.2% of United States electricity [2]. The energy in data centers is mainly consumed by two parts: IT equipment (e.g., servers, storage, network, etc.) and infrastructure (e.g., cooling system). The latter usually accounts for about half of the total energy consumption in a typical data center [3]. As a result, nearly 1% of the electricity is consumed by data center cooling in the United States.

Data center cooling is provided by a dynamic energy system with both system-level and equipment-level controls. Typically, the cooling system consists of water and air loops, various heat and mass transfer equipment, electrical and control devices. The time constants of the data center cooling system vary from seconds (e.g., control system) to hours (e.g., thermal storage). Their time evolution can be described in the continuous time domain, the discrete time domain, and the discrete event domain [4]. Furthermore, the data center cooling system interacts with both inside and outside conditions, such as varying IT loads and local weather conditions. When, where and how the workload is executed in the data center has significant influence on the cooling system [5]. The local weather conditions also impact the efficiency and operational states of the data center cooling systems [6, 7]. Jones [8] outlined seven strategies and directions that should lead to improved energy efficiency of data centers, including the use of dynamic controls for the IT load and cooling system.

Many conventional building performance simulation tools have been exploited to model the energy flow in a data center. Pan et al. [9] developed an energy simulation model for two office buildings with data centers in EnergyPlus [10] to evaluate potential retrofit energy savings. Kummert et al. [11] modeled and analyzed the system inertia of a data center cooling system using TRNSYS [12]. Kuei-Peng et al. [13] applied eQUEST developed with the DOE-2 framework to explore the airside free cooling energy efficiency of data centers in 17 worldwide climate zones.

The conventional simulation tools, however, have exposed several challenges in modeling, simulating and optimizing data center cooling systems. Modeling data center cooling systems may result in a large, complex system model. Managing such large and complex models with these conventional tools can be difficult and time consuming [14]. In addition, those tools have limited capacity when it comes to control designs and evaluations. For instance, EnergyPlus adopts idealized controls to reduce computation time. Although TRNSYS has dynamic control models, its constant time step poses numerical challenges [15]. Further, conventional tools often intertwine model equations and numerical solvers in their source codes; this makes it difficult to extend these programs to support control-oriented cases [16]. Although many case studies have been conducted for data center cooling systems using those tools, they focused on either cooling equipment/system design and retrofit [17-20] or thermal management in the data center room [21-24]. According to the authors' knowledge, there is no case study focusing on the evaluation of the control of the cooling system (such as dead band settings) in an actual data center cooling system. The data center has a large constant internal load, while the office building's cooling load changes over time. This different load profile makes the operation of the data center cooling system different than the other building cooling system and provides a unique opportunity for controls evaluation and optimization.

The equation-based, object-oriented language Modelica [25] can be used to address the abovementioned issues [26]. The Modelica Buildings library has been developed to support various use cases related to Heating Ventilation and Air Conditioning (HVAC) systems in buildings [26, 27]. The Buildings library is an open-source, free library with component and system models for building energy and control systems. The library is also accompanied by Python modules that can be used to automate simulations and post-processing of simulation results.

Besides the conventional energy analysis, this library can also support rapid prototyping [28, 29], modeling of arbitrary HVAC system topologies [28], model-based optimal control [6, 7], evaluation of the stabilization of feedback control and fault detection and diagnostics at the whole building system level [14, 30, 31], and coupled simulation between the cooling system and the room airflow [32-34].

This paper aims to conduct a case study applying Modelica Buildings library to evaluate the dynamic cooling system for a data center located at the University of Massachusetts Medical School in Massachusetts, United States. In this case study, we demonstrate two benefits of Modelica-based modeling: fast prototyping by hierarchical modeling approach, dynamic evaluations of discrete control involving delay time and dead band. The whole paper is organized as follows: Section 2 gives a detailed description of the analyzed cooling and control systems, including the system configurations and different control strategies. Section 3 shows the management of the complex, large system model through a hierarchical modeling approach. The Modelica models are then calibrated using on-site measurement data in Section 4. In Section 5, we first identify several energy and control related issues in the baseline system through an annual simulation. Then we propose different energy efficiency measures (EEMs) to address the identified issues. A sequential search technique is applied to identify the combination of the most cost-effective EEMs in terms of energy savings and life cycle cost (LCC). After that, an optimization of the supply air temperature for the best EEMs is performed to evaluate the energy saving potentials. Conclusions are presented in Section 6.

2 System Description

The data center analyzed operates 24 hours per day, 365 days per year. The data center room has a floor area of 687 m^2 with a white space height of 3.35 m. The room contains 138 IT racks and 12 floor-mounted power distribution units. This case study only focuses on the cooling and control system, and the room-side air distribution management is not considered.

2.1 Cooling System

A primary-only chilled water system with airside economizers (ASEs) is used to provide cooling for the data center room, as shown in Figure 1. The size of detailed components is listed in Table 1. The current cooling load of the data center is about 316 kW. Two identical water-cooled chillers with a design coefficient of performance (COP) of 5.8 work in a Lead/Lag configuration to equalize their runtime. Each chiller has two variable-speed compressors. Two identical cooling towers with variable-speed fans eject the heat from the condenser water loop to the environment. Two chilled water pumps operate with variable speed drives, while two condenser water pumps work at a constant speed. Two Air Handler Units (AHUs) provide cool air to the data center white space. Each AHU consists of an array of 12 variable-speed supply air fans arranged in a parallel-flow configuration. The cool supply air is delivered to cold aisles through an underfloor plenum. The hot IT exhaust air is directed into open hot aisles, then enters a ceiling plenum, then mixing box, and finally returns to the AHUs. When the weather conditions allow, the ASEs are activated to mix the cold outdoor air and warm indoor air to provide precooling or free cooling. The activation and deactivation of ASEs are controlled by a cooling mode controller discussed in Section 2.2.

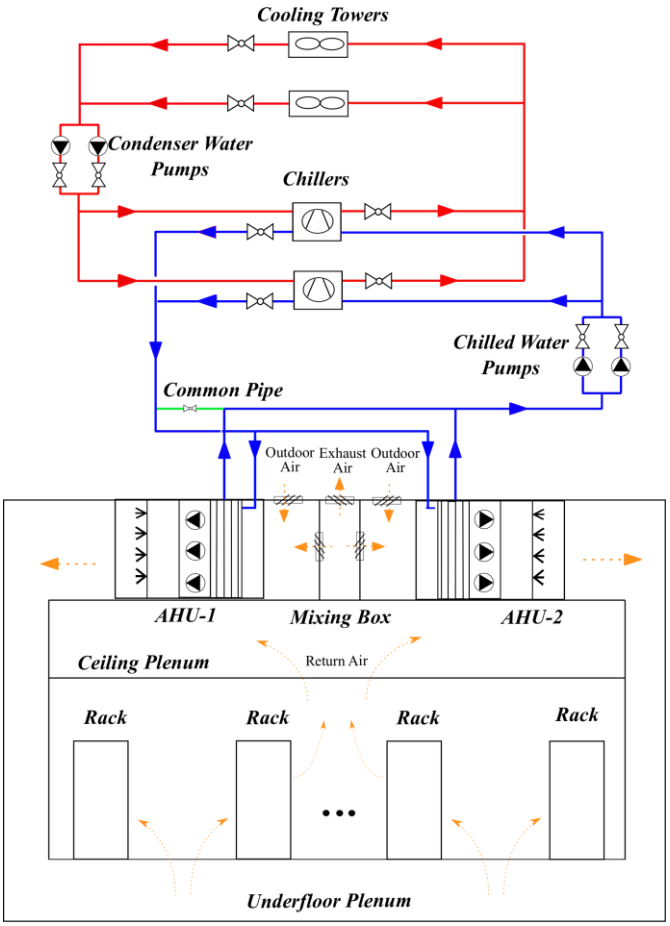

Figure 1. Schematic drawing of the cooling system in the data center

Table 1. Nominal information of components in the cooling system

Equipment	Qty.	Nominal Equipment Information		Unit	Value
AHU	2	Cooling Coil	Air Flowrate	m^3/s	39.2
			Cooling Capacity	kW	696
			Sensible Heat Ratio	-	0.99
			Water Flowrate	kg/s	0.025
		Heating Coil	Qty.	-	4
			Power	kW	31.2
		Steam Humidifier	Qty.	-	4
			Capacity	kg/s	0.019
		Fan	Qty.	-	12
			Head	Pa	622
			Power	kW	3.42
			Flowrate	m^3/s	3.26
Chiller	2	Nominal Capacity		kW	774
		Design COP		-	5.8
		Evaporator	Flowrate	m^3/s	0.028

			Design Outlet Temperature	℃	10
		Condenser	Flowrate	m^3/s	0.026
			Design Inlet Temperature	℃	29.4
		Compressor	Number	-	2
			Speed Type		Variable Speed
			Power	kW	67
Chiller Water Pump	2	Head		mH_2O	41
		Power		kW	12
		Flowrate		m^3/s	0.028
		Speed Type			Variable Speed
Condenser Water Pump	2	Head		mH_2O	29.5
		Power		kW	8
		Flowrate		m^3/s	0.026
		Speed Type			Constant Speed
Cooling Tower	2	Nominal Capacity		kW	893
		Design Approach Temperature		K	4.4
		Number of Cells		-	1
		Number of Fans		-	1
		Fan Speed Type			Variable Speed

2.2 Control System

The control system is composed of a system-level cooling mode control and an equipment-level control with various controllers, as shown in Figure 2. The solid lines show the hierarchical relationship between different controls. The dashed arrows describe the actual control signal flow between different controls. Based on the operational status and outdoor air conditions, the cooling mode controller selects a particular cooling source from the three available choices: chillers only, ASEs only, or both chillers and ASEs. The signal from the cooling mode controller is then sent to the equipment-level controllers to determine the appropriate operating point of individual equipment.

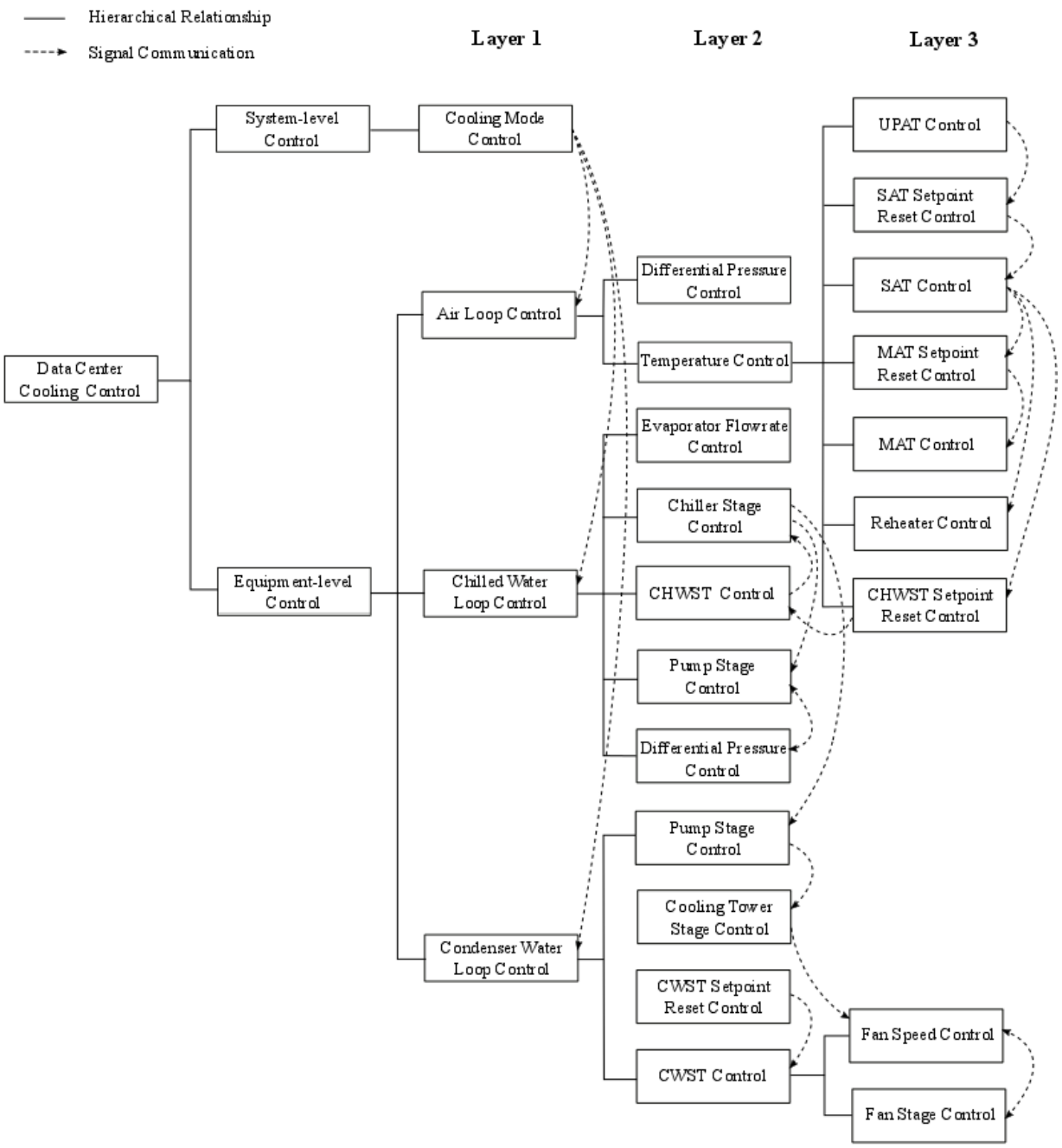

Figure 2. Structure of the data center cooling control

2.2.1 System-level Control

The chilled water system with ASEs can operate in three cooling modes to provide cooling for the data center: (1) Free Cooling (FC) mode, where only ASEs are activated; (2) Partial Mechanical Cooling (PMC) mode, where chillers and ASEs work simultaneously; and (3) Fully Mechanical Cooling (FMC) mode, where only chillers are utilized. As the cooling system has to operate 24 hours per day, 365 days per year, the system "off" state is not considered. The staging among the

different cooling modes is controlled by prescribed transition conditions, which is described by a state graph shown in Figure 3.

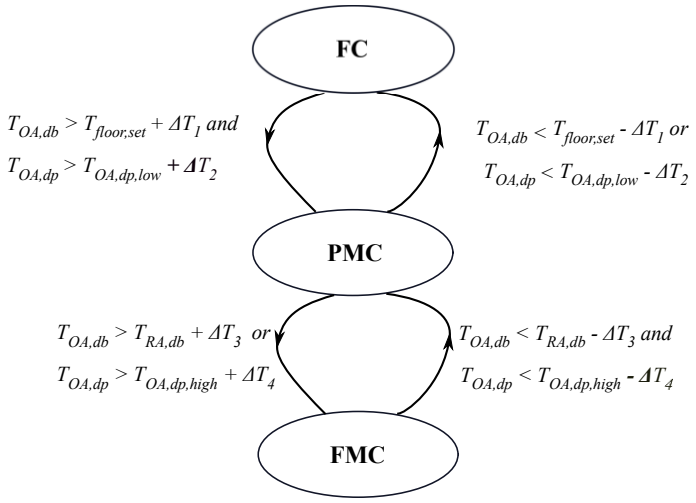

Figure 3. State graph of the cooling mode controller

The transition between FC and PMC mode is determined by air temperature setpoint in the underfloor plenum $T_{floor,set}$ and outdoor air conditions, such as dry bulb temperature, $T_{OA,db}$, and dew point temperature $T_{OA,dp}$.The cooling system switches from FC to PMC mode, when

$$T_{OA,db} > T_{floor,set} + \Delta T_1 \text{ and } T_{OA,dp} > T_{OA,dp,low} + \Delta T_2, \quad (1)$$

and from PMC to FC mode when

$$T_{OA,db} < T_{floor,set} - \Delta T_1 \text{ or } T_{OA,dp} < T_{OA,dp,low} - \Delta T_2 , \quad (2)$$

where $T_{OA,dp,low}$ is the low cutoff limit for $T_{OA,dp}$, and ΔT_1 and ΔT_2 are temperature dead band settings.

The transition between PMC and FMC mode is governed by $T_{OA,db}$, $T_{OA,dp}$, and data center return air temperature $T_{RA,db}$. The cooling system switches from PMC to FMC mode when the following conditions are triggered:

$$T_{OA,db} > T_{RA,db} + \Delta T_3 \text{ or } T_{OA,dp} > T_{OA,dp,high} + \Delta T_4, \quad (3)$$

and from FMC to PMC mode, when the following conditions are met:

$$T_{OA,db} < T_{RA,db} - \Delta T_3 \text{ and } T_{OA,dp} < T_{OA,dp,high} - \Delta T_4, \quad (4)$$

where $T_{OA,dp,high}$ is the high cutoff limit for $T_{OA,dp}$, and ΔT_3 and ΔT_4 are temperature dead band settings. The $T_{OA,dp}$, $T_{OA,db}$, and $T_{RA,db}$ are read from measured data. The $T_{floor,set}$, $T_{OA,dp,high}$ and $T_{OA,dp,low}$ are set to 22.2 ℃, 12.75 ℃, and 11.65 ℃, respectively. The dead bands ΔT_1 and ΔT_3 are set to 1.1 ℃, and ΔT_2 and ΔT_4 are 0.55 ℃. To prevent short-cycling, all the conditions must remain true for 2 minutes before switching to next state.

2.2.2 Equipment-level Control

As shown in Figure 2, the equipment-level control consists of multiple layers with complicated interactions among different controllers. Layer 1 is designed to coordinate the operation of the three major fluid loops of the cooling system: air, chilled water, and condenser water. Each loop has multiple groups of different controls in Layer 2. For instance, the air loop has two groups of controls. One is to control the differential pressure in the underfloor plenum to ensure that a reasonable amount of air passes through the perforated tiles to the data center room. The other is designed for the temperature control. Some groups in Layer 2 also have multiple controllers (Layer 3) dedicated to different control objectives. For example, the condenser water supply temperature (CWST) control in the condenser water loop consists of controls for cooling tower fan staging and fan speed. The details are explained in a top-down approach from Layer 1 to Layer 3 as follows.

2.2.2.1 Air Loop Control

Air loop control includes the control for the underfloor plenum and AHUs. The average static pressure in the underfloor plenum is controlled at a setpoint of 12.4 Pa by modulating the AHU fan speed. The AHUs run all the time. The fans in each AHU are equipped with variable frequency drives and they are controlled to run at the same speed.

The temperature control in the air loop determines the supply air temperature (SAT) setpoint for AHUs, mixed air temperature (MAT) setpoint, outdoor air damper position, chilled water supply temperature (CHWST) setpoint, and control signals for the reheaters in the AHUs. The control strategies and interactions are schematically shown in Figure 4. The underfloor plenum air temperature (UPAT) is maintained at its setpoint $T_{floor,set} = 22.2$ ℃ by resetting the SAT setpoint for AHUs in a range from 15.6 ℃ to 23.3 ℃ using:

$$y = \begin{cases} y_{ref,1}, & u < u_{ref,1} \\ (u - u_{ref,1})\dfrac{y_{ref,2} - y_{ref,1}}{u_{ref,2} - u_{ref,1}} + y_{ref,1}, & u_{ref,1} \le u \le u_{ref,2} \\ y_{ref,2}, & u > u_{ref,2} \end{cases} \quad (5)$$

where u and y are input and output signals respectively. The $u_{ref,1}$, $u_{ref,2}$, $y_{ref,1}$, and $y_{ref,2}$ are predefined reference values. In this case, u is the output of a proportional-integral-derivative (PID) controller (PID-1) and $u_{ref,1} = 0$, $u_{ref,2} = 1$, $y_{ref,1} = 23.3$ ℃, and $y_{ref,2} = 15.6$ ℃. It is worth mentions that (5) is also used by other controllers in Figure 4 but with different reference values for both input and output signals.

Using the reset SAT setpoint and measured SAT, two PID controllers (PID-2 and PID-3) are adopted to control the SAT for AHU-1 and AHU-2, respectively. The output signal y_2 and y_3 from the two PID controllers, ranging from 0 to 1, are then used in different control strategies under different cooling modes.

- In the FC mode, the SAT is maintained at its setpoint by adjusting the MAT setpoint. The maximum of the output signals y_2 and y_3 is used to reset the MAT setpoint within a range of 14.4 ℃ to 25.3 ℃ through (5). The MAT is then maintained at its setpoint by adjusting the outdoor air dampers through a PID controller (PID-4).

- In the PMC and FMC modes, the system will either reset the CHWST setpoint or activate reheaters to maintain the SAT. To reset the CHWST setpoint, the output signals y_2 and y_3 are mapped to the CHWST setpoint within the range of 7.8 ℃ to 12.2 ℃. The minimum of the mapped setpoints $CHWST_{set,1}$ and $CHWST_{set,2}$ is then sent to the chillers as the CHWST setpoint. For the reheaters, y_2 and y_3 are mapped to a control signal ranging from 0 to 1 in order to adjust the power of reheaters in AHU-1 and AHU-2, respectively. Take AHU-1 as an example. The reference values in the CHWST setpoint reset control are set to $u_{ref,1}$= 0.4, $u_{ref,2}$ = 1, $y_{ref,1}$ = 12.2 ℃ and $y_{ref,2}$ = 7.8 ℃. In the reheater control, they are set to $u_{ref,1} = 0$, $u_{ref,2} = 0.4$, $y_{ref,1} = 1$ and $y_{ref,2} = 0$. When the output signal y_2 of PID-2 is less than 0.4, the CHWST setpoint reset control is deactivated, and the reheater control is activated. Reverse actions are triggered when y_2 is greater than 0.4.

2.2.2.2 Chilled Water Loop

Chilled water loop control is composed of controls for the chillers and chilled water pumps. At the current cooling load, only one chiller is needed when FMC or PMC mode is activated. The chilled water pumps are set up to run one pump per chiller. The speed of the chilled water pumps is modulated by a PI controller to maintain a constant pressure difference of 206 kPa between the inlet and the outlet of the chiller evaporators. The bypass valve in the common leg is regulated by a PI controller to maintain a constant flowrate through the evaporators.

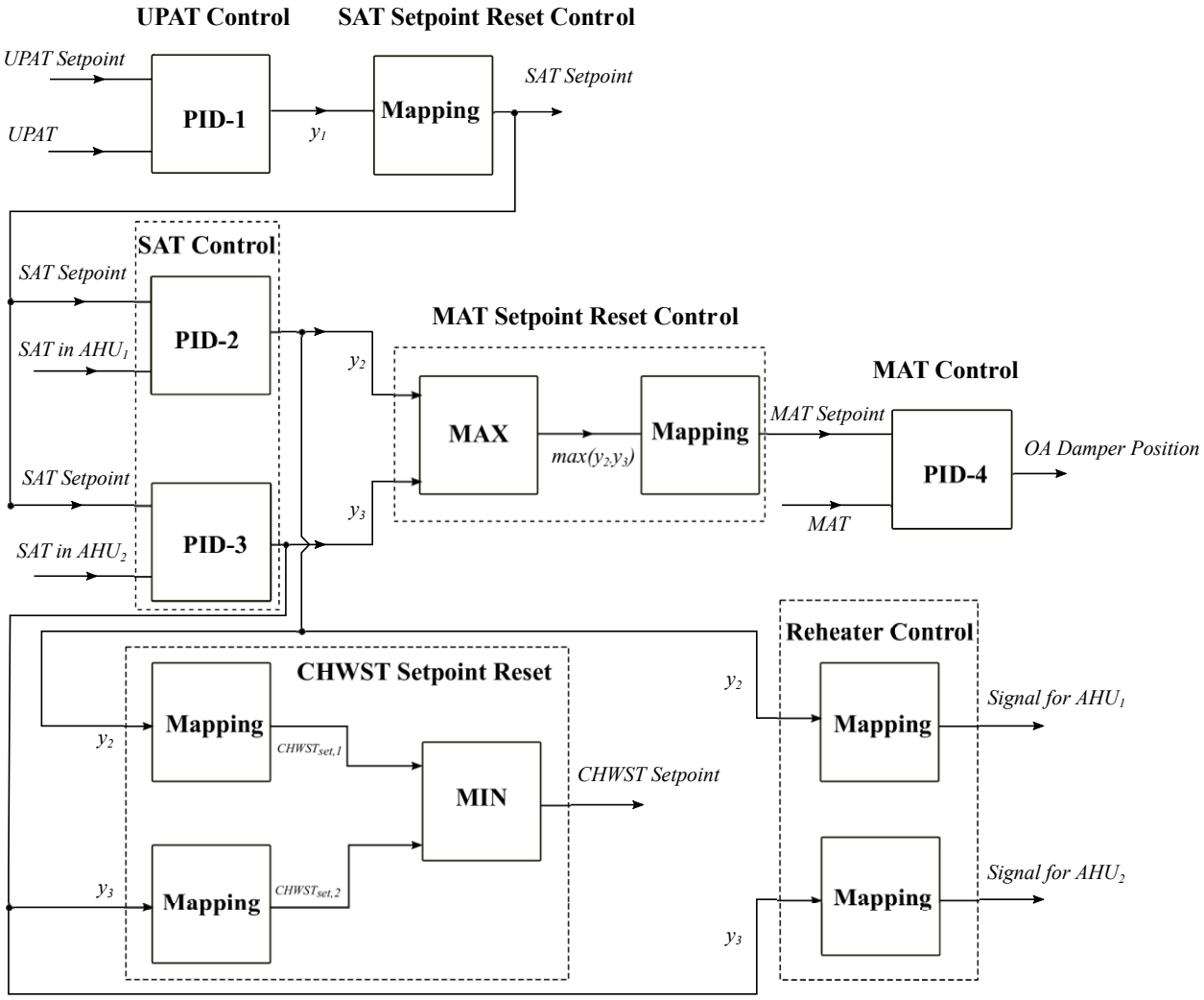

Figure 4. Temperature control for the air loop

2.2.2.3 Condenser Water Loop

Condenser water loop control includes controls for the condenser water pumps and cooling towers. The condenser water pumps and cooling towers are staged based on the number of operating chillers: one condenser water pump and cooling tower is commanded on if one chiller is required. The CWST setpoint is reset from 21.1 ℃ to 29.4 ℃ as the outdoor air wet bulb temperature increases from 17.2 ℃ to 25.6 ℃ using the mapping algorithm in (5).

The speed and number of operating fans in cooling towers are manipulated to control the CWST at its setpoint. The fan speed is adjusted by a PI controller to reduce the difference between the CWST and the setpoint, and the number of working fans is determined as follows:

One additional fan is switched on if

$$T_{cws} > T_{cws,set} + \Delta T, and\ SP_{fan} > SP_{high} + \Delta SP, \quad (6)$$

and switched off if

$$T_{cws} < T_{cws,set} - \Delta T, or\ SP_{fan} < SP_{low} - \Delta SP, \quad (7)$$

where T_{cws} is condenser water supply temperature, $T_{cws,set}$ is condenser water supply temperature setpoint, ΔT is temperature dead band, SP_{fan} is cooling tower fan speed, SP_{high}, SP_{low} are the high and low threshold of the fan speed,, and ΔSP is the fan speed dead band. In this case study, ΔT is set to 1 ℃, SP_{high} is set to 0.8, SP_{low} is set to 0.4, and ΔSP is set to 0.1. To prevent short-cycling, the conditions described in (6) an (7) need to remain true for 5 minutes before the control actions are triggered.

3 Modelica Models

The cooling and control systems are modeled using the Modelica language. The Modelica Buildings library version 5.0.0 provides models for data center cooling systems [35]. The following sections illustrate how to perform modeling and simulation by taking advantage of object-oriented, equation-based modeling. We first introduce the implementation of equipment models and control system models, and then demonstrate the system model by integrating the models of equipment and control.

3.1 Component Models for the Cooling System

Most components of the cooling system are modeled directly using the existing models in the Modelica Buildings library. The pipes and ducts are modeled using *Buildings.Fluid.FixedResistances.PressureDrop*, which is a flow resistance with a fixed flow coefficient. The cooling tower is modeled using *Buildings.Fluid.HeatExchangers.CoolingTowers.YorkCalc*, which uses a polynomial to predict the approach temperature for the cooling tower at off-design conditions. The performance of chiller compressor is predicted using the DOE-2 electrical chiller model [36], which consists of 3 performance curves: CAPFT – a curve that represents available cooling capacity as a function of the evaporator and condenser temperature, EIRFT – a curve that represents the full load efficiency as function of the evaporator and condenser temperature, and EIRFPLR – a curve that represents the efficiency as a function of the part-load ratio. The head and power of the pumps/fans are represented as a quadratic equation in terms of the flowrate. Detailed curves are shown in Table 2, where T_{wb} is the wet bulb temperature, T_{ran} is the range temperature defined as the temperature difference between the supply and return condenser water, r is the water to air mass flowrate ratio, T_{chws} is the chilled water supply temperature, T_{cws} is the condenser water supply temperature, PLR is the part load ratio, Q is the flowrate of water or air, H is the head of the pump/fan, P is the power of the pump/fan. a, b, c, d, e, f are the coefficients that needed to be calibrated for each model.

For component models that are not included in the Buildings library, we constructed the models based on Modelica standard library (Version 3.2.2 Build 3) and Buildings library (Version 5.0.0). For example, the Buildings library has no model for a chiller that is equipped with two variable-speed compressors. However, such a dual-compressor chiller model can be built quickly by utilizing the existing chiller models in the Buildings library. As shown in Figure 5, we instantiated an electric chiller object model (*Buildings.Fluid.Chillers.ElectricEIR*) twice to represent two variable-speed compressors, denoted as “Compressor 1” and “Compressor 2”, respectively. Each compressor has its own performance curves to calculate the off-design performance.

Table 2. Performance curves for major cooling equipment

Model	Performance Curves
Cooling Tower	$T_{app} = a_1 + a_2 T_{wb} + a_3 T_{wb}^2 + a_4 T_{ran} + a_5 T_{ran} T_{wb} + a_6 T_{wb}^2 T_{ran} + a_7 T_{ran}^2 + a_8 T_{wb} T_{ran}^2 + a_9 T_{wb}^2 T_{ran}^2 + a_{10} r + a_{11} T_{wb} r + a_{12} T_{wb}^2 r + a_{13} T_{ran} r + a_{14} T_{wb} T_{ran} r + a_{15} T_{wb}^2 T_{ran} r + a_{16} T_{ran}^2 r + a_{17} T_{wb} T_{ran}^2 r + a_{18} T_{wb}^2 T_{ran}^2 r + a_{19} r^2 + a_{20} T_{wb} r^2 + a_{21} T_{wb}^2 r^2 + a_{22} T_{ran} r^2 + a_{23} T_{wb} T_{ran} r^2 + a_{24} T_{wb}^2 T_{ran} r^2 + a_{25} T_{ran}^2 r^2 + a_{26} T_{wb} T_{ran}^2 r^2 + a_{27} T_{wb}^2 T_{ran}^2 r^2$
Chiller	$CAPFT = b_1 + b_2 T_{chws} + b_3 T_{chws}^2 + b_4 T_{cws} + b_5 T_{cws}^2 + b_6 T_{chws} T_{cws}$ $EIRFT = c_1 + c_2 T_{chws} + c_3 T_{chws}^2 + c_4 T_{cws} + c_5 T_{cws}^2 + c_6 T_{chws} T_{cws}$ $EIRFPLR = d_1 + d_2 PLR + d_3 PLR^2$
Pump/Fan	$H = e_1 + e_2 Q + e_3 Q^2$ $P = f_1 + f_2 Q + f_3 Q^2$

A stage control is also included to activate the compressors based on load conditions and other control commands. When the chiller is commanded on, one compressor will be turned on immediately. The second compressor is staged on if

$$T_{chws} > T_{chws,set} + \Delta T, and\ \Delta t_{off} > \Delta t_{thr}\ , \tag{8}$$

and staged off if

$$T_{chws} < T_{chws,set} - \Delta T, and\ \Delta t_{on} > \Delta t_{thr} \tag{9}$$

where T_{chws} is the chilled water supply temperature, $T_{chws,set}$ is the chilled water supply temperature setpoint, ΔT is a temperature dead band of 1 ℃, Δt_{off} is the elapsed time since the compressor was off, Δt_{on} is the passing of time after the compressor was commanded on last time, and Δt_{thr} is the time threshold (e.g. 20 minutes in this case) to prevent short cycling of compressors.

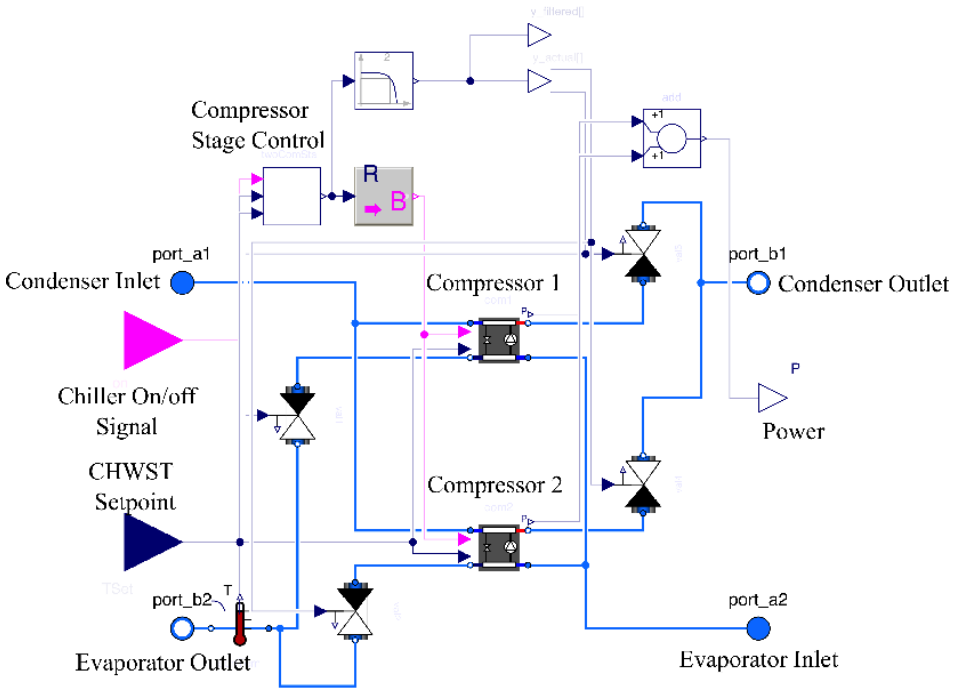

Figure 5. Diagram of Modelica model for a chiller with two variable speed compressors

3.2 Control System Model

3.2.1 Cooling Mode Control

Figure 6 shows the Modelica implementation of the cooling mode control described in Figure 2. On the left are the connectors for the control input signals expressed as real numbers, including $T_{floor,set}$, $T_{OA,db}$, $T_{OA,dp}$, and $T_{RA,db}$. In the middle is the state graph implemented using the Modelica state graph package. On the right are signal conversions from Boolean to Integer signals, followed by an Integer connector, which outputs the control signal of the cooling modes.

There are three states in the cooling mode controller, indicated by the squared block icons in the middle of Figure 6. The states are FC, PMC, and FMC mode. The initial state is set to FMC mode when simulation starts. The transitions between the states are represented by the horizontal black bars, and each transition has exactly one preceding state and one succeeding state.

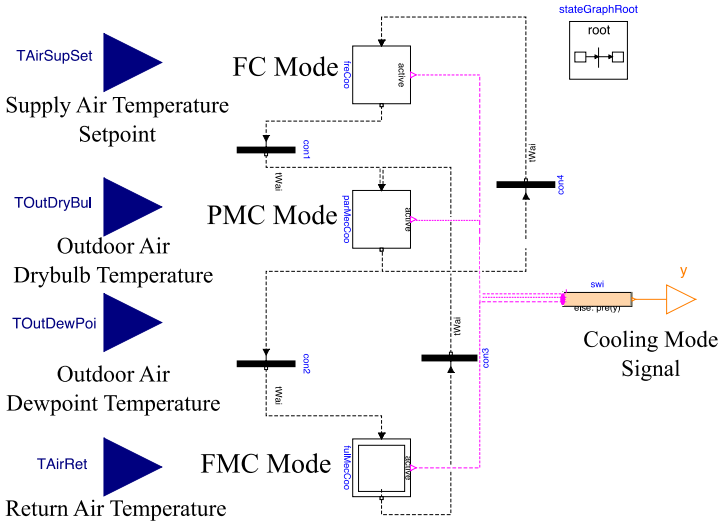

Figure 6. Diagram of Modelica models for the cooling mode control

3.2.2 Equipment-Level Controls

The hierarchy of the equipment-level controls described in **Error! Reference source not found.** is implemented in Modelica by a bottom-up approach. We first declare the equipment controls at Layer 3 as Modelica classes. Then we instantiate these classes and encapsulate their instances layer by layer (from Layer 3 to Layer 1) to formulate the control models for the different loops in Layer 1.

Figure 7 shows a part of the hierarchical models of the condenser water loop control. Each icon encapsulates a model that may encapsulate other models. Figure 7(a) shows the model for the condenser water loop control in Layer 1, including pump stage control, cooling tower stage control, CWST setpoint reset control, and CWST control, as indicated in the dash boxes. Figure 7(b) shows the implementation of CWST control in Layer 2. The CWST control model further encapsulates the instantiations of fan stage control model and the fan speed control model in Layer 3. For instance, Figure 7(c) demonstrates the implementation of the fan speed control model. Taking advantages of object inheritance, and instantiation in the object-oriented Modelica, this hierarchical modeling structure allows users to manage the complexity of large models, and to assemble system models as one would connect components in an actual system. This structure also facilitates debugging and verification of component models. For example, a lower-level model is first debugged and verified, and then instantiated in a higher-level model, which can help identify modelling errors at the early stage of the model development.

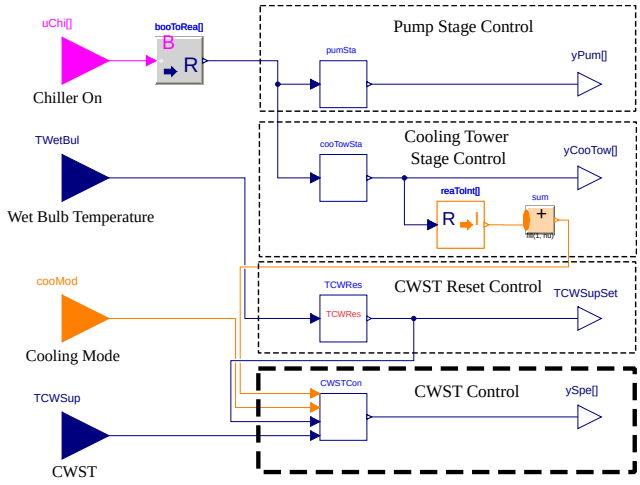

(a) Diagram of the condenser water loop control

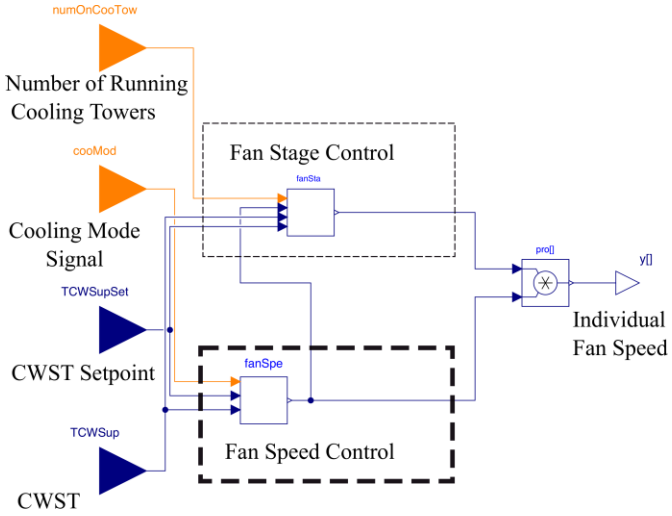

(b) Diagram of the CWST control in the condenser water loop control

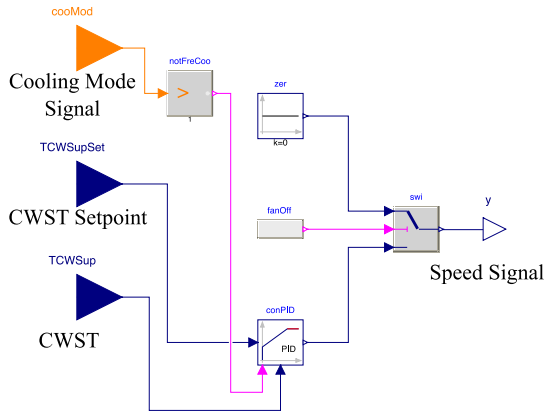

(c) Diagram of the fan speed control in the CWST control

Figure 7. Hierarchical Modelica models of the condenser water loop control

3.3 System Models

After implementing the necessary equipment and control models, this section introduces the system model which combines both the physical plant and control system. Several important assumptions are made to simplify the system level model. First, the cooling load in the data center room consists of only heat generation from IT equipment. The heat transfer from envelope and lighting are not considered. Second, the cooling load in the data center is assumed to be constant and equally distributed into two zones (158 kW in each zone). Each zone is cooled by a separate AHU. This assumption is reasonable because the measured heat transfer and power for the two AHUs are almost identical. Third, each zone is modeled as an ideally-mixed volume by assuming the air in the data center room to be completely mixed, because our focus here is the backend cooling system instead of air flow distribution in the room. Forth, the underfloor plenum is modeled using a lumped resistance model instead of a detailed air flow model. Last, communication and computation in the control system are assumed to be instantaneous.

As shown in Figure 8, the integrated system model is composed of two parts: the cooling system and the control system. The cooling system is shown at the right side, where the red solid lines represent the condenser water loop, the blue solid lines represent the chilled water loop, and the yellow lines represent the air loop. The controls are displayed on the left side of Figure 8, and include the cooling mode control, and equipment-level controls such as the condenser water loop control, the chilled water loop control, and the air loop control.

Each component model that formulates the system model is verified in a simulation example following the procedure used by the Modelica Buildings library [26]. We validated the customized models using analytical verification, which has also been used to validate all individual component models in the Modelica Buildings library. For example, the model for the chiller with two variable-speed compressors is verified by comparing its simulation results with the analytical solutions that are derived for certain steady-state or transient boundary conditions.

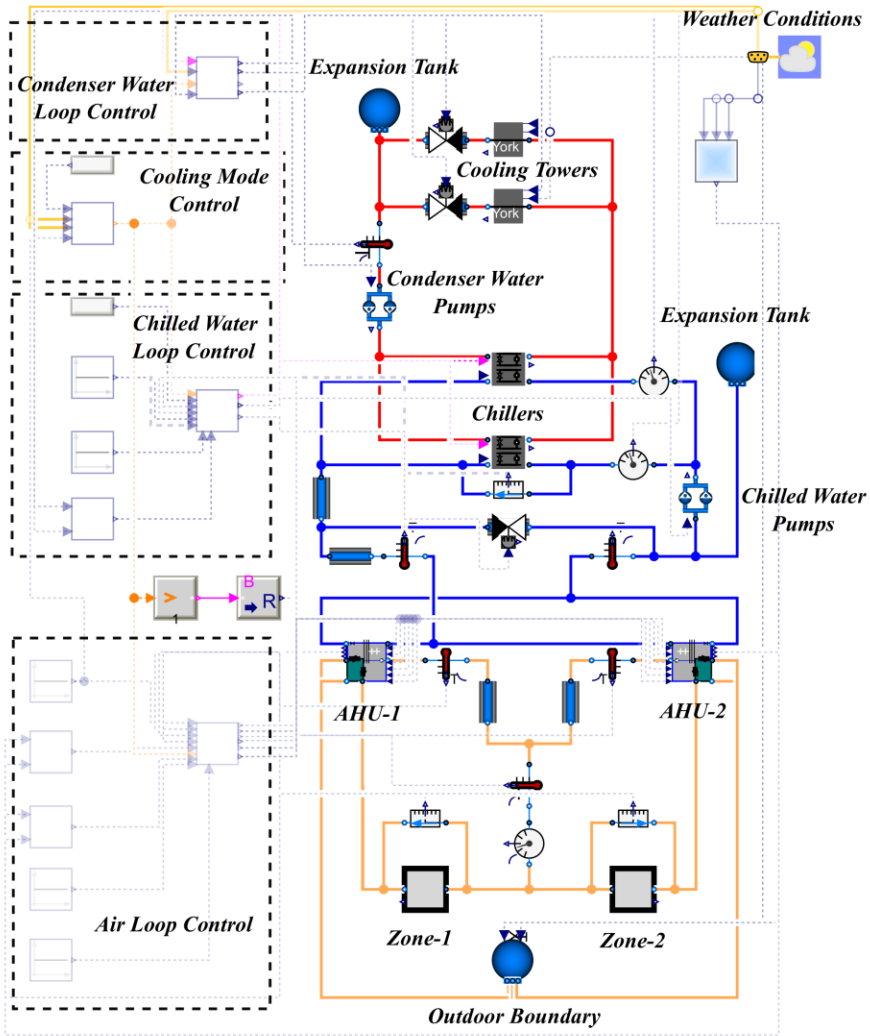

Figure 8. Implementation of the system-level model in Modelica

4 Calibration

To evaluate the performance of potential retrofit solutions, we need to establish a baseline model which will predict the performance of the data center cooling system. Figure 9 describes a general procedure to calibrate the baseline model. To automate the calibration process, we formulated it as an optimization problem. The objective of the calibration is to minimize the difference between the model output and the corresponding measurement. The difference is defined by the Normalized Mean Bias Error (NMBE), e_{NMBE}. The formulation of the optimization problem is shown in (10).

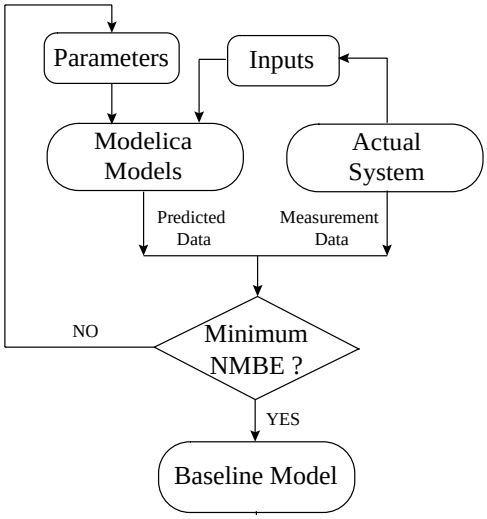

Figure 9. Flowchart of the baseline model calibration

$$\min\ (e_{NMBE}) = \min\left(\frac{\int_{t_0}^{t_0+\Delta t} |f(p,in,t) - M(t)|dt}{\int_{t_0}^{t_0+\Delta t} |M(t)|dt}\right),$$
$$s.t.\ p_{lb} \le p \le p_{ub}, \tag{10}$$

where f is the calibrated model, which are shown in Table 3. M is the corresponding measurement, in are the inputs for the Modelica models, which can be obtained from measurement data, t_0 and Δt are initial time and length of the calibration period, p are the adjustable parameters of the model, and p_{lb} and p_{ub} are the lower and upper bounds of the parameters p, respectively. The optimization problem is solved using the Particle Swarm Optimization algorithm [37] in GenOpt .

To calibrate the baseline model, the abovementioned optimization problem was established and solved for each cooling equipment using measurement data from October 3 to November 3 in 2017. The measurement data were sampled at a 5-minute interval and divided into two sets: the first 80% were used for calibrating the models, and the remaining 20% were used to evaluate the calibrated models. Table 3 shows the calibration problems and their results for different equipment. The AHUs are calibrated by adjusting nominal UA values ($UA_{nominal}$) to predict the outlet temperatures on both air and water side. For the chiller, since the chiller needs two compressors to run at the same time at current cooling load level and we only have the measurement data for the chiller as a whole, we assume the two compressors have the same performance during the calibration. Because the condenser water pump runs at constant speed and the measured power is almost constant, we only calibrated the nominal power ($P_{nominal}$) and nominal head ($H_{nominal}$) instead of the performance curves listed in Table 3.

Relative errors between measurement and prediction are within 8% for all component models during calibration and evaluation. The system electricity consumption error during the calibration and evaluation period is obtained as 5% and 6% after the calibration of the component models.

Although only limited measurement data are utilized for calibration, it is sufficient enough to predict for other seasons. The reasons are listed as follows. First, at the early October, the outdoor

air temperature is high enough for the system to run at mechanical cooling (PMC and FMC) mode, while at the late October the system can work at FC mode. The measurement data might be in a broad range for calibration. Second, when the mechanical cooling (PMC and FMC) is activated, the performance of chiller is calibrated using the inlet condenser water temperature (T_{cws}), the outlet evaporator temperature (T_{chws}). Because both temperatures are controlled within a limited range during the whole year, and the measurement in October covers most of the range (see Table 3), it is acceptable to use measurement in October to calibrate chillers. Similar situation happens for pumps and cooling coils in AHUs. For the cooling tower, although the wet bulb temperature in October is much higher than that in February, but it has little influence on the performance of the cooling tower, because in cold days, the cooling towers are shut off.

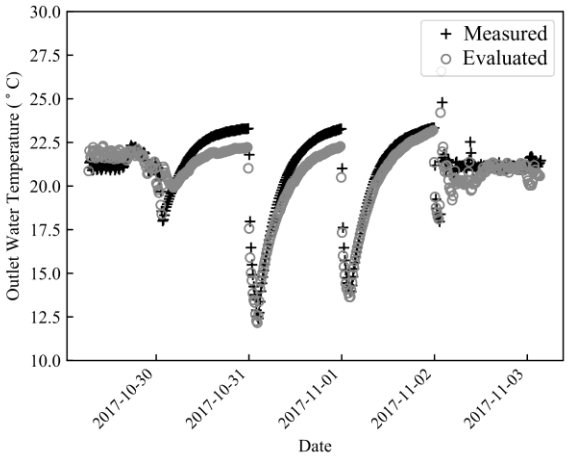

Figure 10. Evaluation results for cooling towers

1 Table 3. Calibration and evaluation results

Model		Input	Range	Adjusted Parameters	Calibrated Results	Relative Errors	
						Calibration	Evaluation
AHU-1		$T_{wat,in}$	[8, 12.1] ℃	$UA_{nominal}$	28.6 kW/K	7%	3%
		$T_{air,in}$	[24.2, 28.1] ℃				
AHU-2		m_{wat}	[12.5, 14.5] kg/s	$UA_{nominal}$	30.2 kW/K	8%	3%
		m_{air}	[30.3, 37.7] kg/s				
Chiller	Compressor 1 /Compressor 2	T_{chws}	[8, 12.1] ℃	b_i	[1.002148,3.300191E-02,3.741670E-04,-5.925358E-03,-2.599267E-05,-2.172126E-04]	8%	6%
		T_{cws}	[21.2, 25.8] ℃	c_i	[4.475957E-01,-1.054652E-02,7.126870E-04,1.158632E-02,5.151510E-04,-9.831355E-04]		
		PLR	[0.35, 0.56]	d_i	[2.519108E-01,2.756914E-01,4.725826E-01]		
Cooling Tower		T_{wb}	[1.8, 22.0] ℃	a_i	[-2.3982747E-01,-3.6702405E-02,1.590029E-03,1.15951251E-01,-1.6564918E-02,3.22868E-04,-3.726566E-03,3.84672E-04,-8.94952E-06,1.898438674,-8.1176766E-02,9.73283E-04,1.120285767,-1.1128052E-02,-4.79369E-04,-1.699013E-02,3.24994E-05,1.81282E-05,-4.3584417E-02,-1.518778E-03,1.66684E-04,-6.0704364E-02,2.121175E-03,2.57478E-05,-2.285692E-03,5.7106E-06,1.01121E-06]	4%	4%
		T_{ran}	[3.3, 7.8] ℃				
		r	[0.9, 1.8]				
Chilled Water Pump		Q	[0.02, 0.03]m^3/s	e_i	[7.66E05, 1.74E07, 8.58E06]	2%	3%
				f_i	[9.20, 4.21E05, 6.82E06]		
Cooling Tower Fan		SP	[0.5, 1]	e_i	N/A	3%	3%
				f_i	[0,0,0,7.23789E03]		
Condenser Water Pump		N/A	N/A	$P_{nominal}$	8.623E03 W	1%	1%
				$H_{nominal}$	2.89288E05 Pa		

2

5 Retrofit Solutions

We first performed an annual numerical simulation of the baseline system. Based on the analysis of the energy and control performance, we identified several control related issues and proposed corresponding design solutions to improve the control performance. The new design solutions were then examined using the system models. Lastly, we conducted an optimization to further improve the energy saving potentials of the proposed solutions. All the simulations were performed using the local weather data in 2017.

5.1 Baseline System

The simulation of the baseline system with calibrated equipment models and control settings shows that the cooling system works in FC, PMC, and FMC modes for 6310, 17, and 2433 hours in 2017, respectively. We identified three potential improvements in terms of control and energy efficiency.

First, the cooling coils are degraded possibly because of fouling. The calculated overall thermal conductance according to the measured data is $UA = 28.6$ kW/K for the AHU-1, which is only 37% of the design value ($UA = 77.4$ kW/K) calculated from the manufacture data.

Second, the simulation results show that the cooling system generally operates either in FMC mode or FC mode. However, it rarely works in PMC mode, where the return air is pre-cooled by cold outdoor air. The cooling mode control are defined in (1) to (4). However, the difference between $T_{OA,dp,low}$ in (2) and $T_{OA,dp,high}$ in (3) is only 1.1 ℃, which is small. As a result, the system will be able to stay in PMC mode only if $T_{OA,dp}$ is between 12.2 ℃ and 13.3 ℃. Otherwise, it will move to FMC or FC mode.

Third, there is simultaneous heating and cooling in the AHUs, which is caused by the control of the SAT and the chilled water flow rate as described in Section 2.2.2. In FMC mode, it is possible that the SAT is lower than the set point (e.g. the control output signal y_2 from PID-2 is less than 0.4). This will activate the reheaters in AHU-1, but the CHWST will remain the same because the chiller CHWST reset control can only be activated when y_2 is larger than 0.4. As a result, the air is overcooled by the chilled water and then heated by reheaters in AHU-1. Besides the SAT control, lacking flow rate control for the chilled water in AHUs also contributes to the simultaneous heating and cooling problem. As described in Section 2.2.2, the speed of the primary pumps is modulated to maintain a fixed pressure difference of 206 kPa between the inlet and outlet of the evaporators, and the bypass valve is adjusted to guarantee that the chilled water through the evaporators is 0.03 m^3/s all the time. Without direct control of the chilled water through the cooling coils, it can lead to a persistent oversupply or undersupply of chilled water to the cooling coils. The oversupply of chilled water can over-cool the supply air.

5.2 Energy Efficiency Measures

To address the energy inefficiencies identified above, we propose the following three energy efficiency measures (EEMs) for the cooling and control systems. The rest of this paper uses "M" to represent the system with the corresponding EEMs implemented.

5.2.1 M_1: Clean Cooling Coils

In system M_1, we propose cleaning the fouled cooling coils on both water and air sides. We assume that the UA value of the cleaned cooling coils can be the same as the design nominal UA value. However, the simulation results show that cleaning the cooling coil alone actually results in 76%

more energy consumption than the baseline results because improving the cooling efficiency makes the existing over-cooling problem even worse. After being cleaned, the heat transfer effectiveness of the cooling coils increases, which means under the same CHWST, the cleaned cooling coils cool the supply air to a lower temperature than the fouled cooling coils. As a result, the AHUs with clean cooling coils need additional reheat energy to maintain the same SAT when the water flowrate through the cooling coils is not regulated. For example, when $T_{floor,set}$ is reset to 23.3 ℃, the CHWST can be as high as 12.2 ℃. The fouled cooling coils can cool the supply air to around 21.0 ℃, and we just need to reheat it to 23.3 ℃. However, the clean cooling coils can cool the supply air to around 18.0 ℃, and additional energy is expended to bring the SAT to 23.3 ℃. Furthermore, the energy of chillers and cooling towers in M_1 increases because the heat generated by the reheaters increases the thermal load of the chillers and hence cooling towers.

5.2.2 M_2: Improve Cooling Mode Control

To increase the operating time of PMC mode, we need to make it easier to move from FMC to PMC and more difficult to move back. To achieve this goal, we propose to increase the $T_{OA,dp,high}$ by setting it to 15 ℃ in system M_2. This temperature is a high $T_{OA,dp}$ recommended by ASHRAE for the data center equipment environment [38]. All the other settings remain the same as the baseline system.

The annual simulation show that M_2 can save 9.0% of cooling energy compared to the baseline system because the improved cooling mode controller allows the cooling system to operate less in FMC mode, and more in FC and PMC modes. The detailed explanation is as follows:

- The higher cutoff limit of $T_{OA,dp}$ (15 ℃) reduces the operational time of FMC mode in M_2 (from 2,433 hours to 1,632 hours). Due to a higher $T_{OA,dp}$, the system can stay in PMC mode longer. As a result, M_2 operates in PMC mode for 188 hours in the whole year, compared to 16 hours for the baseline system. As the chillers only need to address part of the cooling load in PMC mode, they consume less energy than in FMC mode.
- More importantly, M_2 works in FC mode for 6,938 hours, which is 628 hours more than the baseline system. By increasing the time staying in PMC mode, it also increases the possibility of switching from PMC mode to FC mode. For example, as shown in Figure 11, the baseline system works in FMC mode all the time from July 12 to July 15, but M_2 can work in FC mode for almost two days in the same period. The $T_{OA,db}$ is lower than $T_{floor,set}$ as well as $T_{RA,db}$ during most of the time. At the beginning of July 12, $T_{OA,dp}$ is higher than the high dew point temperature cutoff limit in both the baseline system ($T_{OA,dp,high,Baseline}$) and M_2 ($T_{OA,dp,high,M_2}$), thus FMC mode is activated in both systems. However, as $T_{OA,dp}$ continues decreasing to $T_{OA,dp,high,M_2}$, M_2 can operate in PMC mode, while the baseline system still works in FMC mode. When M_2 works in PMC mode, (2) is easily triggered because $T_{OA,db}$ is lower than $T_{floor,set}$, which switches the system from PMC to FC mode. Therefore, with a higher $T_{OA,dp,high}$, it is easier for the cooling system to switch from FMC to PMC mode, and then to FC mode.

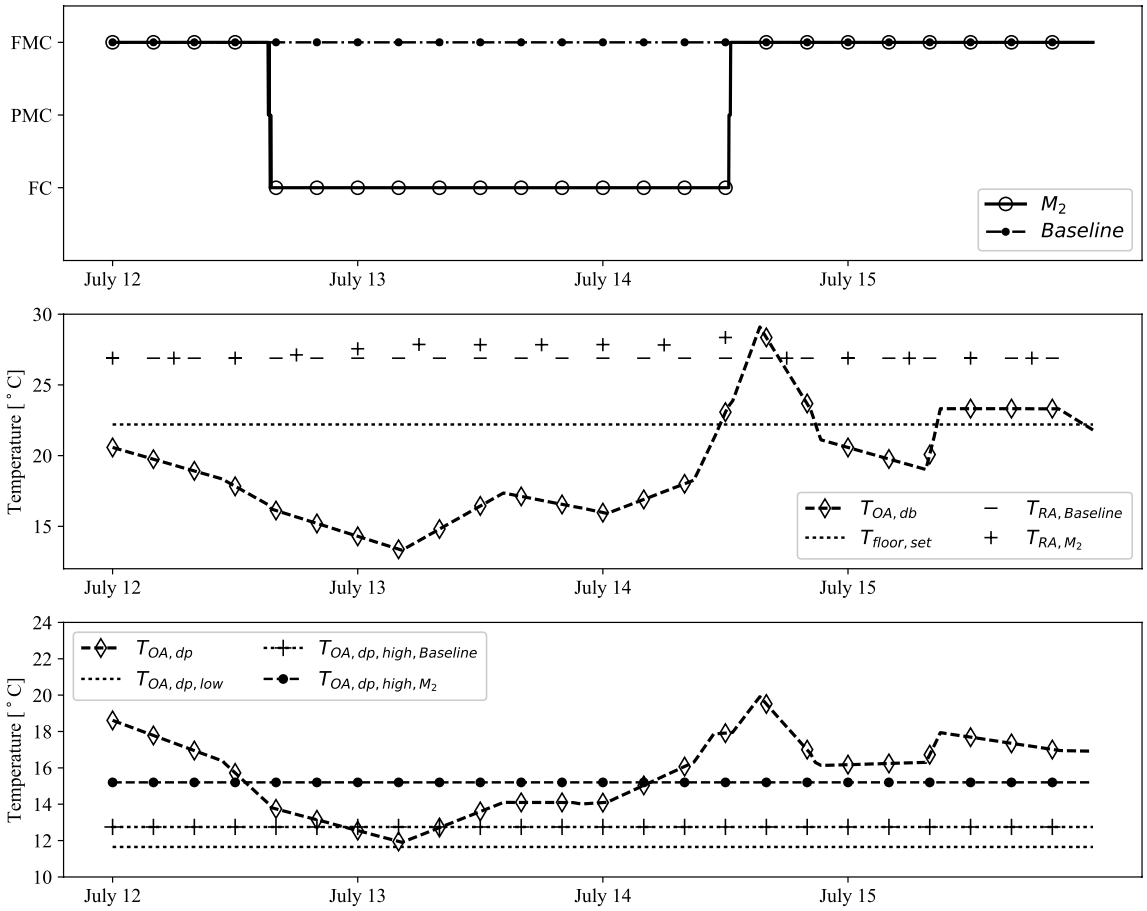

Figure 11. Comparison of the system details in M_2 and the baseline system

However, increasing $T_{OA,dp,high}$ might pose challenges for the humidity control of the underfloor air. Figure 12 shows the box plot of the hourly relative humidity (RH) in both M_2 and the baseline system. The central rectangular box spans the first quartile to the third quartile, and the dashed line inside displays the median. The lower and upper whiskers represent the 0.1 percentile and the 99.9 percentile, respectively, which means there is only 0.1% of the data between the minimum and the lower whisker, and 99.9% of data between the minimum and the upper whisker. In the baseline system, the RH is within the boundary preferred by the operators. However, M_2 exceeds the upper bound since it introduces more humid outdoor air in the data center room for free cooling, and the cooling coil in the AHUs has a very limited capacity for dehumidification with a design sensible heat ratio of 0.99.

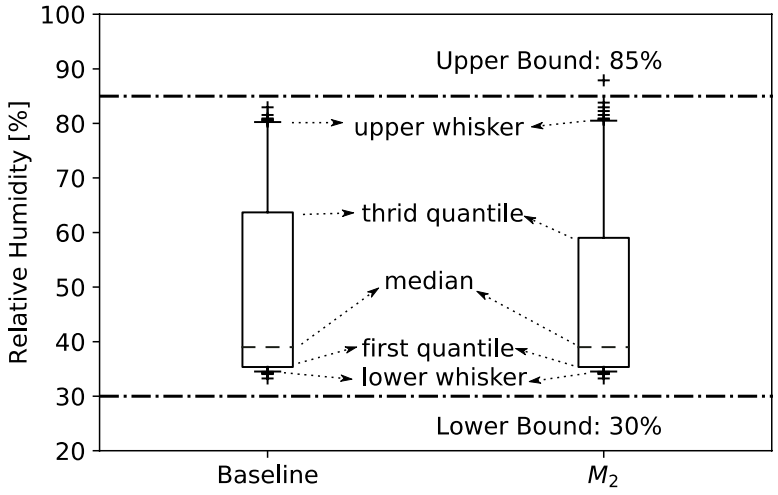

Figure 12. RH of underfloor air in M_2 and the baseline system

5.2.3 M_3: Improve SAT Control

To mitigate the problems of simultaneously heating and cooling in the AHUs, we propose adding a two-way valve on the waterside of cooling coils to regulate to maintain the SAT in PMC and FMC modes in system M_3. Instead of maintaining a constant differential pressure between the inlet and outlet of the evaporators, M_3 adjusts the speed of the primary pumps to maintain a fixed differential pressure of 83 kPa between the inlet and the outlet of the cooling coils. The bypass valve in the common leg is adjusted to achieve a minimum flow rate through evaporators. The above proposal will regulate the amount of chilled water passing through the cooling coils to avoid an oversupply of chilled water and reduce simultaneous heating and cooling in AHUs.

Simulation results show that 9.4% of cooling energy can be saved in M_3. Most of the savings are from reheaters. Figure 13 compares the operational status of M_3 and the baseline system during July 12 to July 15. Although the systems operate in the same cooling mode, to track the same SAT setpoint, the reheaters in the baseline system need to be activated, while those in M_3 are completely deactivated (see the bottom figure in Figure 13).

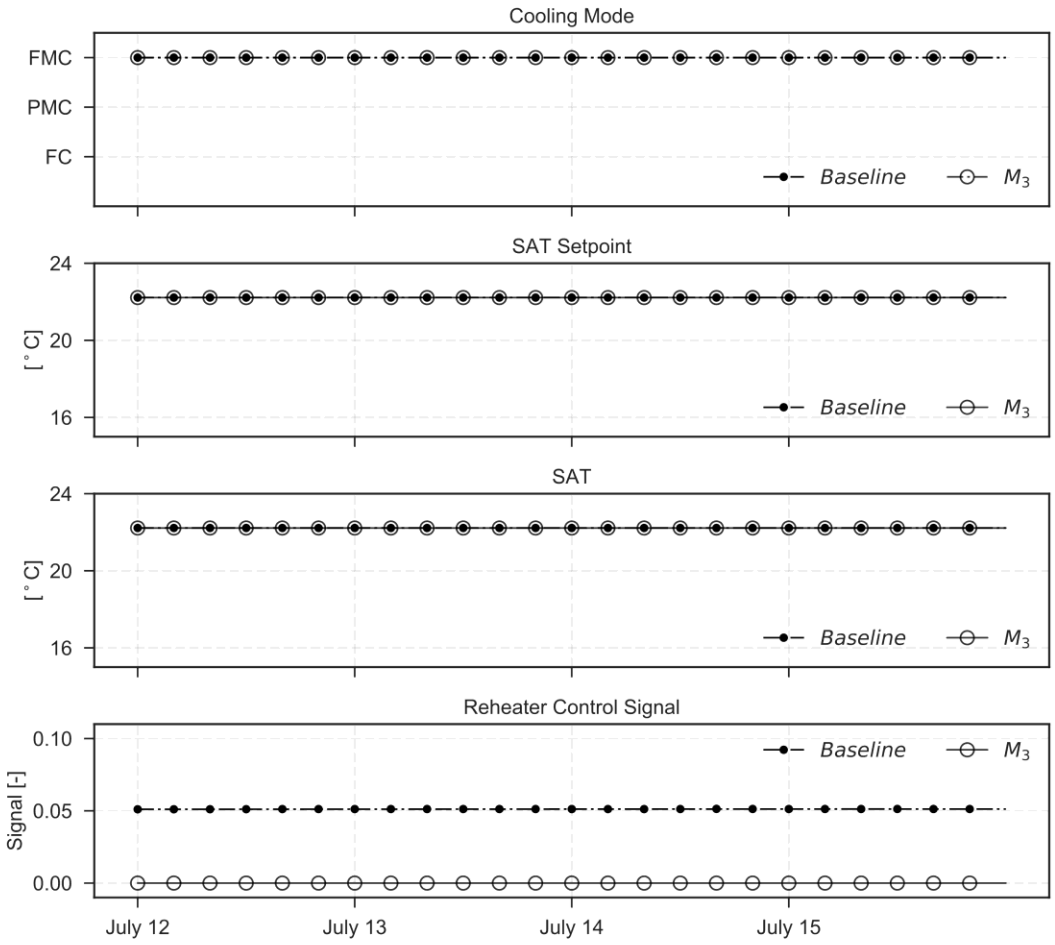

Figure 13. Cooling and heating in the AHUs. Simultaneous heating and cooling is avoided in M_3

5.3 Sequential Search for EEMs

The process of designing and retrofitting real buildings often involves choosing among discrete options, for example, different EEMs. To propose the best EEMs for a building retrofit, engineers need to explore and search the design space of possible EEMs. Genetic Algorithms (GAs) are most commonly used for building energy optimizations [39]. Others seek to develop the Pareto Frontier – the set of cost-optimal solutions over a range of energy savings [40, 41]. However, GAs are typically for optimization problems with large amount of decision variables, such as a large amount of different EEMs. Because we only proposed three EEMs in this case, the Sequential Search Technique [42, 43] is utilized to find the most cost-effective retrofit solutions.

5.3.1 Sequential Search Technique

The basic principle of Sequential Search technique is schematically shown in Figure 14. All the proposed EEMs are simulated individually. These simulations comprise an initial iteration of the optimization process. As illustrated in Figure 14, the most cost-effective option (points with steepest slope compared with the optimal design in previous iteration), based on simulation results and energy-related costs, is chosen as the baseline point for the next iteration. The chosen EEM is then removed from future evaluations by the search. Remaining EEMs are simulated in the

presence of this new baseline point and the iterative process repeats. The method can provide intermediate optimal points, that is, the minimum cost designs at various levels of energy savings, which enables the engineers to make their choice when they are interested in intermediate solutions, rather than a global optimum [42, 43].

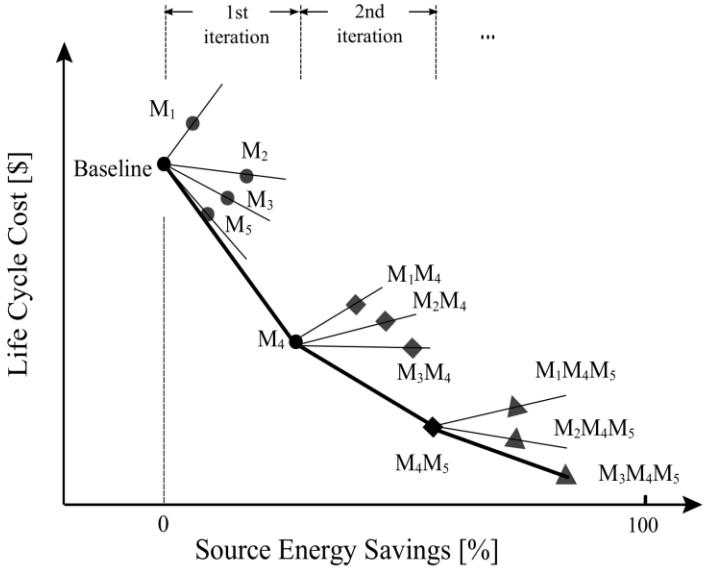

Figure 14. Illustration of Sequential Search Technique

5.3.2 Results of Sequential Search Technique

We performed a sequential search technique among the abovementioned three EEMs considering energy savings and LCC. For energy savings, only electricity consumed by the cooling system was taken into account. The LCC is calculated using Eq. (11). The N is the life cycle, and the r_d is the real discount rate. The $C_{i,n}$, $C_{o,n}$, and $C_{m,n}$ are capital cost, operation cost and maintenance cost in year n, respectively. In this study, we set N to 40 years, and r_d to 0.02. Capital costs for different measures were estimated by experienced engineers of the analyzed data center, and operation costs were calculated using a variable basic service charge offered by the utility company in Massachusetts [44], which is also shown in Table 4. Maintenance cost for each measure was set to 0 in this study.

$$LCC = \sum_{n=1}^{N} \frac{C_{i,n} + C_{o,n} + C_{m,n}}{(1 + r_d)^n} \tag{11}$$

The results of Sequential Search are documented in Table 5. The calculated LCCs are listed in the 6th column, and the energy savings compared with the baseline point of each iteration (optimal solution in previous iteration) are listed in the 7th column. The slopes between the baseline point in each iteration and the evaluated EEMs are shown in the last column, where N/A means the slope is not calculated because the EEM cannot save energy. In Iteration 1, a single EEM is compared with the baseline system. M_2 is identified as the most cost-effective solution and then serves as the baseline point for Iteration 2. The simulation results show that the combination of M_2 and M_3 is better than that of M_1 and M_2, because M_1 cannot save energy at all. In the third iteration, compared

with the new baseline point M_2M_3, the only combination of $M_1M_2M_3$ has no advantage in terms of both energy savings and LCC.

Sequential search among the proposed EEMs shows that M_2 is suggested if one EEM is adopted, and M_2M_3 is suggested if two EEMs are considered. The combination $M_1M_2M_3$ cannot further reduce energy and LCC compared with M_2M_3, and hence is not an effective retrofit option.

Table 4. Utility rates used in the studied data center

Month	Price ($/kWh)	Month	Price ($/kWh)	Month	Price ($/kWh)
January	0.10759	May	0.06823	September	0.08515
February	0.10632	June	0.08505	October	0.08360
March	0.08565	July	0.08993	November	0.08908
April	0.07226	August	0.08752	December	0.10415

Table 5. Sequential search process for the proposed EEMs

Iteration #	EEM	Energy (MWh)	Annual Operation Cost ($)	Initial Cost ($)	LCC ($)	Energy Savings (%)	Slope
1	Baseline	446	39,121	0	1,070,174	0	0
	M_1	787	68,574	1,000	1,876,875	-76.5	N/A
	M_2	406	35,574	100	973,244	8.97	-1,080,768
	M_3	404	35,458	110,037	1,080,008	9.42	104,426
2	Baseline	406	35,574	100	973,244	0	0
	M_1M_2	656	57,208	1,100	1,566,052	-61.6	N/A
	M_2M_3	358	31,481	110,137	971,315	11.8	-16,316
3	Baseline	358	31,481	110,137	971,315	0	0
	$M_1M_2M_3$	358	31,523	111,137	973,464	0	N/A

5.4 Optimal Underfloor Plenum Air Temperature Setpoint

To further investigate the energy saving potentials, we proposed to optimize the cooling system by adjusting the control setpoint of the UPAT in addition to the searched EEMs in Section 5.3. The following section describes the setup and results of the optimization.

5.4.1 Optimization Problem Setup

The optimization problem is formulated as:

$$\min\left(\sum_{con} E_{con}\left(T_{floor,set}\right)\right), \qquad (12)$$

$$s.t.\ \ T_{floor,set,l} \le T_{floor,set} \le T_{floor,set,u}$$

where E is the energy consumption, and the subscript con represents different electricity consumers in the cooling system, including chillers, pumps, cooling towers, and AHUs. The energy consumed by the server fans are considered constant in the optimization problem. The

UPAT setpoint $T_{floor,set}$ is chosen as the only design variable in this case study. The subscript l and u are the lower and upper bound. Here we assume that the rack inlet temperature is the same as the UPAT. Thus, we can set $T_{floor,set,l} = 18$ ℃ and $T_{floor,set,u} = 27$ ℃ based on ASHRAE's recommended range for rack inlet temperatures [38]. The optimization problem is then solved using exhaustive search or parametric analysis with an increment of 0.1 ℃ for the design variable.

5.4.2 Optimization Results

We performed the optimization on three systems: the baseline system, M_2, and M_2M_3. The relationship between the $T_{floor,set}$ and the annual energy consumption for the three systems is shown in Figure 15. The systems with optimal $T_{floor,set}$ are denoted as Baseline_{opt}, $M_{2,opt}$, and $M_2M_{3,opt}$ respectively. The results show that the optimal $T_{floor,set}$ of Baseline_{opt} and $M_{2,opt}$ is 25.1 ℃, and that of $M_2M_{3,opt}$ is 27 ℃. The additional energy savings by optimizing the UPAT are around 20 ~ 25 MWh for all three cases. As a result, the combined energy savings for Baseline_{opt}, $M_{2,opt}$, and $M_2M_{3,opt}$ are 4.5%, 14.6% and 24.2% compared with the baseline system, respectively.

Figure 15 shows that starting from $T_{floor,set} = 18$ ℃, the energy consumption reduces when increasing $T_{floor,set}$. However, for the baseline system and M_2, when $T_{floor,set}$ reaches around 25.1 ℃, the annual energy consumption starts to increase. The reason is that when $T_{floor,set}$ is higher than 25.1 ℃, the increased reheat energy is larger than the savings from the chillers and their associated pumps. For example, for the baseline system (Figure 16), when $T_{floor,set}$ increases from 25.1 ℃ to 27 ℃, the reheat energy in one year increases from 20.4 MWh to 99.0 MWh, but the energy consumed by the chillers only decreases from 89.5 MWh to 87.9 MWh. In M_2M_3, the reheaters consume no energy at all even when $T_{floor,set}$ increases because reheating in the AHUs is avoided.

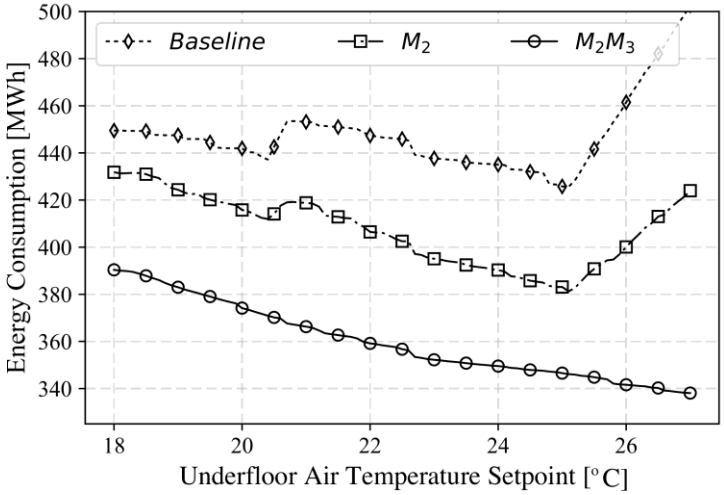

Figure 15. Relationship between $T_{floor,set}$ and annual energy consumption for different systems

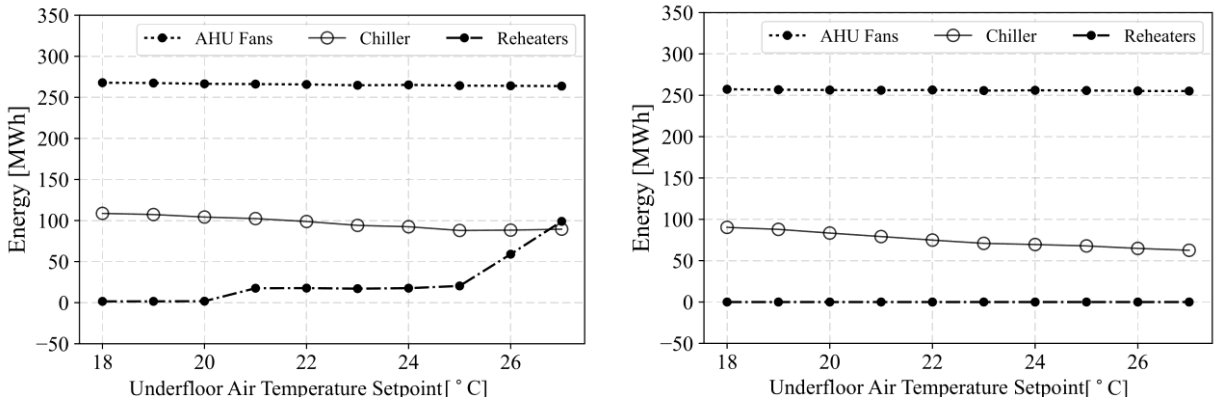

Figure 16. Energy impact of $T_{floor,set}$ on major cooling equipment: (left) baseline system; (right) M_2M_3

It is worth mentioning that the equipment-level control strategies have significant influence on the design space of the above optimization problem. For example, Figure 15 shows that with the baseline reheat control, the baseline system and M_2 have local optima around 20.5 ℃. The local optima are caused by the activation of reheaters in the AHUs. In M_2M_3, the annual energy consumption monotonously decreases as $T_{floor,set}$ increases, because the reheaters are off for the entire range of $T_{floor,set}$.

Figure 17 shows the operating time under different UPATs during the whole year in the baseline system and three optimal systems. The UPATs are controlled at their setpoints with a tolerance of ±1.5 ℃ for about 96% of the year in the baseline system, and about 99% in all three optimized systems.

Figure 18 compares the RH in the underfloor plenum for a whole year in a box plot with whiskers of 0.1 and 99.9 percentile. The RH in all four systems is within the preferred range. The median RHs in the Baseline_{opt}, $M_{2,opt}$, and $M_2M_{3,opt}$ are lower than that in the baseline system, because the RH decreases as the dry bulb temperature increases if the dew point temperature is the same. Taking the baseline system and Baseline_{opt} for example, the only difference is that the Baseline_{opt} utilizes $T_{floor,set}$ =25.1 ℃ instead of 22.2 ℃ in the baseline system. Because these two systems have the same $T_{OA,dp}$ thresholds in the cooling mode controller, and their cooling coils have limited capacity of dehumidification, we can assume these two systems have the same dew point temperature in the underfloor plenum for most time. However, UPAT in $M_{2,opt}$ is controlled at 25.1 ℃, about 3 ℃ higher than the baseline system. Therefore, the median RH in the Baseline_{opt} is lower than the baseline system.

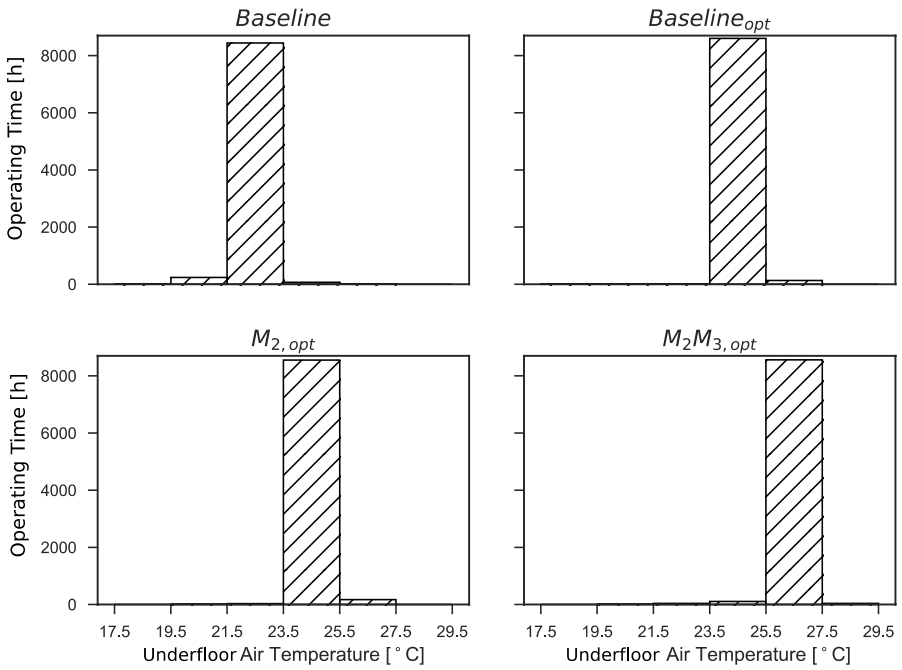

Figure 17. Operating time under different UPATs for four different systems during a year

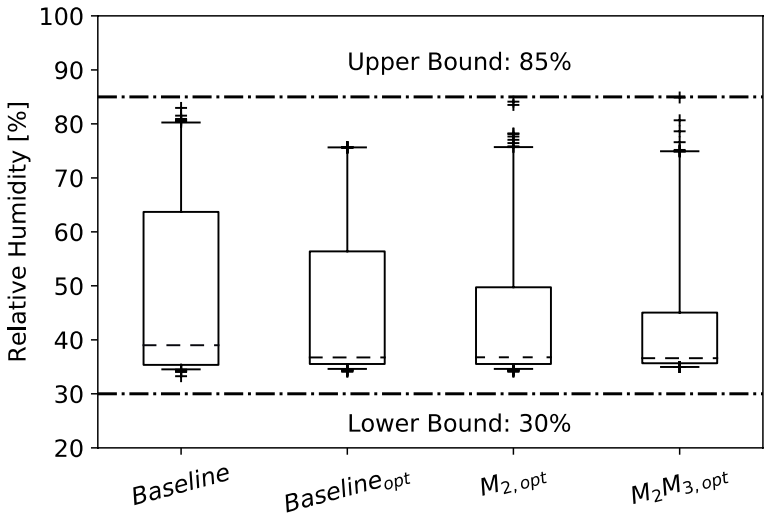

Figure 18. Box plot of the underfloor RH in different systems

To understand when the energy savings are achieved in the three optimal systems, we show detailed analysis in Figure 19. The energy savings in Baseline$_{opt}$, $M_{2,opt}$, and $M_2M_{3,opt}$ mostly take place during transition (e.g. October ~ November) and summer seasons (e.g. September). There

are barely energy savings from winter because of free cooling. The maximum daily energy saving in all cases is about 2000 kWh, where all the mechanical cooling is totally deactivated.

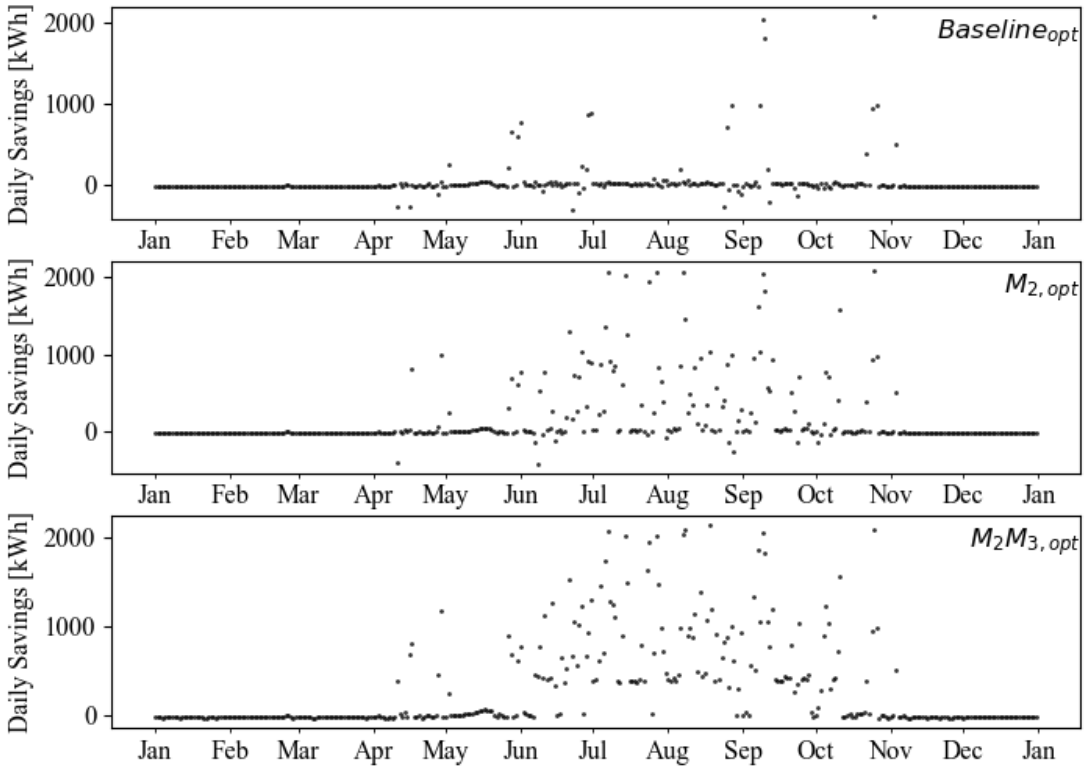

Figure 19. Daily energy savings for different systems

To understand where the energy savings are from, we break down the savings in $Baseline_{opt}$ as an example shown in Figure 20. For a single day, the cooling tower fans can save up to 150 kWh, and all the pumps together can save up to 480 kWh. The largest saving is from deactivation of the chiller, which can reduce energy by about 900 kWh in a day. For the AHUs, due to the increase of $T_{floor,set}$, the fans need to operate at a higher speed to deliver more air to the data center room in order to keep the room at the setpoint. Therefore, during a winter day, the AHU fans in the $Baseline_{opt}$ can consume 10 kWh more energy than the baseline system due to the increase of the fan speed. For the transition and summer seasons, the AHUs in the $Baseline_{opt}$ can save up to 500 kWh if the reheaters are deactivated, but can also consume about 500 kWh more energy if the reheaters are triggered due to the control in Section 2.2.2.1.

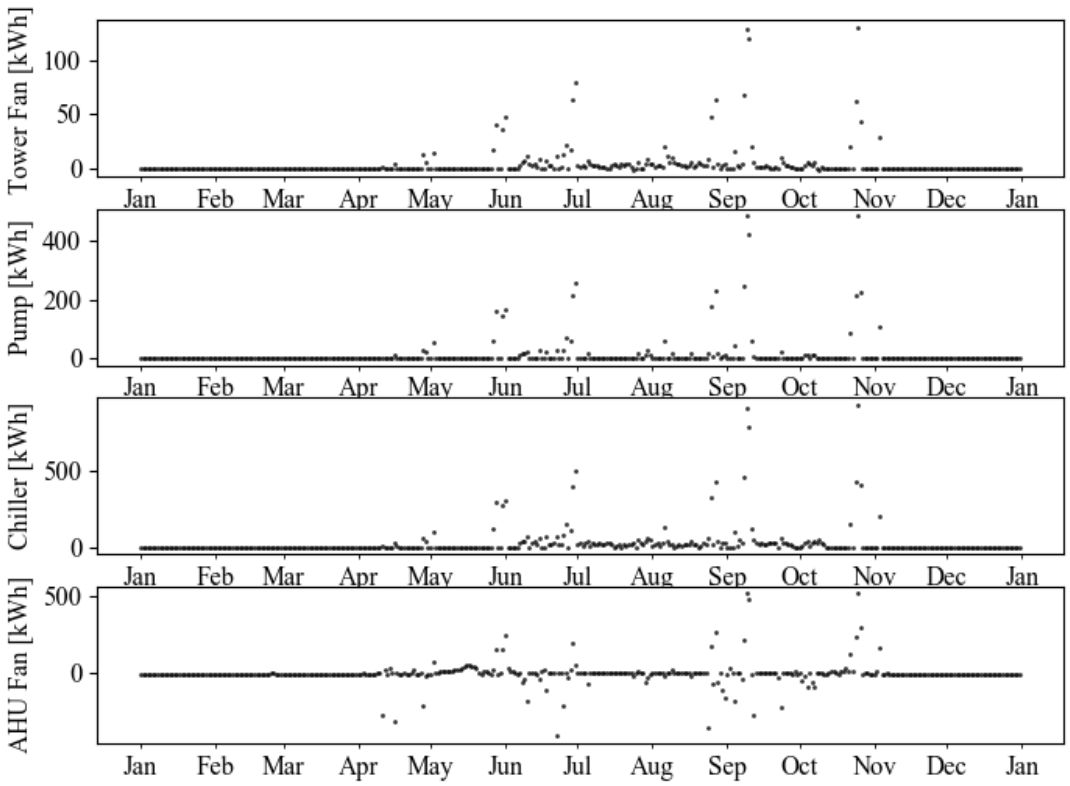

Figure 20. Daily energy savings in $Baseline_{opt}$

6 Conclusions

In the present study, an equation-based dynamic modeling and simulation approach is performed to evaluate energy and control performance, to develop EEMs, and to optimize the operation in a medium-size data center located in Massachusetts, United States. The baseline cooling and control systems is built in Modelica and calibrated using measurement data. Three individual EEMs related to energy and dynamic control performance are proposed: (M_1) cleaning the cooling coils in the AHUs; (M_2) increasing high cutoff limit of outdoor air dew point temperature in cooling mode controller; (M_3) improving AHU controls to avoid simultaneous heating and cooling.

The intermediate cost-effective retrofit solutions among the proposed EEMs are then identified through the Sequential Search technique. If only one EEM is adopted when budget is limited, M_2 is suggested due to its low initial cost and considerable energy savings. If two EEMs are considered, M_2 and M_3 together can save up to 19.7% cooling energy. Adopting three EEMs simultaneously is not recommended in this case, because it is hardly a cost effective retrofit.

In the end, by optimizing the underfloor air temperature setpoint in addition to the proposed EEMs, the data center can potentially save as much as 24.2% energy for the cooling system with M_2 and M_3 adopted. The optimal settings for the cooling system can maintain the data center room in an acceptable thermal environment in terms of temperature and relative humidity. The energy savings for all the optimized systems come from summer and transition seasons.

This case study also demonstrates two important features in Modelica-based tools. One is the capability of complexity management through hierarchical modeling, which supports fast modeling of various user cases. The other is the ability to evaluate discrete control involving delay time and dead band, which are commonly used in the control of the cooling system.

7 Acknowledgement

This research is financially funded by U.S. Department of Energy under the award NO. DE-EE0007688. This work was also supported by the Assistant Secretary for Energy Efficiency and Renewable Energy, the U.S. Department of Energy under Contract No. DE-AC02-05CH11231.

8 Reference

1. Dayarathna, M., Y. Wen, and R. Fan, *Data center energy consumption modeling: A survey.* IEEE Communications Surveys & Tutorials, 2016. **18**(1): p. 732-794.
2. Koomey, J., *Growth in data center electricity use 2005 to 2010.* A report by Analytical Press, completed at the request of The New York Times, 2011. **9**.
3. Van Heddeghem, W., et al., *Trends in worldwide ICT electricity consumption from 2007 to 2012.* Computer Communications, 2014. **50**: p. 64-76.
4. Wetter, M., *A view on future building system modeling and simulation*. 2011, Ernest Orlando Lawrence Berkeley National Laboratory, Berkeley, CA (US): United States.
5. Parolini, L., *Models and control strategies for data center energy efficiency*. 2012, Carnegie Mellon University.
6. Huang, S., W. Zuo, and M.D. Sohn, *Amelioration of the cooling load based chiller sequencing control.* Applied Energy, 2016. **168**: p. 204-215.
7. Huang, S., W. Zuo, and M.D. Sohn, *Improved cooling tower control of legacy chiller plants by optimizing the condenser water set point.* Building and Environment, 2017. **111**: p. 33-46.
8. Jones, R., *Seven strategies to improve data center cooling efficiency*. 2008, The Green Grid White Paper.
9. Pan, Y., R. Yin, and Z. Huang, *Energy modeling of two office buildings with data center for green building design.* Energy and Buildings, 2008. **40**(7): p. 1145-1152.
10. Crawley, D.B., et al., *EnergyPlus: energy simulation program.* ASHRAE journal, 2000. **42**(4): p. 49.
11. Kummert, M., W. Dempster, and K. McLean. *Transient thermal analysis of a data centre cooling system under fault conditions*. in *11th International Building Performance Simulation association Conference and Exhibition, Building Simulation 2009*. 2009.
12. Klein, S.A., *TRNSYS-A transient system simulation program.* University of Wisconsin-Madison, Engineering Experiment Station Report, 1988: p. 38-12.
13. Lee, K.-P. and H.-L. Chen, *Analysis of energy saving potential of air-side free cooling for data centers in worldwide climate zones.* Energy and Buildings, 2013. **64**: p. 103-112.

14. Wetter, M., *Modelica-based modelling and simulation to support research and development in building energy and control systems.* Journal of Building Performance Simulation, 2009. **2**(2): p. 143-161

15. Kim, D., et al. *Comparisons of building system modeling approaches for control system design*. in *Proceedings of the 13th International Conference of the International Building Performance Simulation Association (Building Simulation 2013)*. 2013.

16. Wetter, M., M. Bonvini, and T.S. Nouidui, *Equation-based languages–A new paradigm for building energy modeling, simulation and optimization.* Energy and Buildings, 2016. **117**: p. 290-300.

17. Cho, J., T. Lim, and B.S. Kim, *Viability of datacenter cooling systems for energy efficiency in temperate or subtropical regions: Case study.* Energy and buildings, 2012. **55**: p. 189-197.

18. Kim, J.-Y., et al., *Energy conservation effects of a multi-stage outdoor air enabled cooling system in a data center.* Energy and Buildings, 2017. **138**: p. 257-270.

19. Siriwardana, J., S. Jayasekara, and S.K. Halgamuge, *Potential of air-side economizers for data center cooling: A case study for key Australian cities.* Applied Energy, 2013. **104**: p. 207-219.

20. Choo, K., R.M. Galante, and M.M. Ohadi, *Energy consumption analysis of a medium-size primary data center in an academic campus.* Energy and Buildings, 2014. **76**: p. 414-421.

21. Ahuja, N., et al. *Data center efficiency with higher ambient temperatures and optimized cooling control*. in *Semiconductor Thermal Measurement and Management Symposium (SEMI-THERM), 2011 27th Annual IEEE*. 2011. IEEE.

22. Fakhim, B., et al., *Cooling solutions in an operational data centre: A case study.* Applied thermal engineering, 2011. **31**(14-15): p. 2279-2291.

23. Hamann, H.F. *A measurement-based method for improving data center energy efficiency*. in *Sensor Networks, Ubiquitous and Trustworthy Computing, 2008. SUTC'08. IEEE International Conference on*. 2008. IEEE.

24. Hamann, H.F., V. López, and A. Stepanchuk. *Thermal zones for more efficient data center energy management*. in *Thermal and Thermomechanical Phenomena in Electronic Systems (ITherm), 2010 12th IEEE Intersociety Conference on*. 2010. IEEE.

25. Fritzson, P., *Principles of object-oriented modeling and simulation with Modelica 2.1*. 2010: John Wiley & Sons.

26. Wetter, M., et al., *Modelica buildings library.* Journal of Building Performance Simulation, 2014. **7**(4): p. 253-270.

27. Wetter, M., et al. *Modelica buildings library 2.0*. in *Proc. of The 14th International Conference of the International Building Performance Simulation Association (Building Simulation 2015), Hyderabad, India*. 2015.

28. Wetter, M., *A Modelica-based model library for building energy and control systems.* Lawrence Berkeley National Laboratory, 2010.

29. He, D., et al., *Towards to the development of virtual testbed for net zero energy communities.* Proceedings of SimBuild, 2016. **6**(1).

30. Eisenhower, B., K. Gasljevic, and I. Mezic, *Control-oriented dynamic modeling and calibration of a campus theater using Modelica.* SimBuild 2012, 2012.

31. Lee, D., B. Lee, and J.W. Shin. *Fault Detection and Diagnosis with Modelica Language using Deep Belief Network*. in *Proceedings of the 11th International Modelica Conference, Versailles, France, September 21-23, 2015*. 2015. Linköping University Electronic Press.

32. Tian, W., et al. *Optimization on Thermostat Location in an Office Room Using the Coupled Simulation Platform in Modelica Buildings Library: A Pilot Study*. in *2018 COBEE conference*. 2018.

33. Tian, W., et al., *Coupling fast fluid dynamics and multizone airflow models in Modelica Buildings library to simulate the dynamics of HVAC systems.* Building and Environment, 2017. **122**: p. 269-286.

34. Tian, W., et al. *Coupled Simulation between CFD and Multizone Models Based on Modelica Buildings Library to Study Indoor Environment Control*. in *Proceedings of the 12th International Modelica Conference, Prague, Czech Republic, May 15-17, 2017*. 2017. Linköping University Electronic Press.

35. Fu, Y., M. Wetter, and W. Zuo, *Modelica Models for Data Center Cooling Systems*. Conference: 2018 ASHRAE Building Performance Analysis Conference and SimBuild (BPACS 2018)), September 26-28, Chicago, IL. 2018: ; University of Colorado Boulder. Medium: ED.

36. Hydeman, M. and K.L. Gillespie, *Tools and techniques to calibrate electric chiller component models.* ASHRAE transactions, 2002. **108**(1): p. 733-741.

37. Kennedy, J., *Particle swarm optimization*, in *Encyclopedia of machine learning*. 2011, Springer. p. 760-766.

38. Committee, A.T., *ASHRAE TC 9.9 Thermal guidelines for data processing enviroments*. 2011, USA: American Society of Heating, Refrigerating and Air Conditioning Engineers Inc.

39. Wetter, M., *Simulation-based building energy optimization*. 2004, University of California, Berkeley.

40. Wang, W., R. Zmeureanu, and H. Rivard, *Applying multi-objective genetic algorithms in green building design optimization.* Building and environment, 2005. **40**(11): p. 1512-1525.

41. Feng, F., et al., *Optimizing the topologies of heating, ventilation, and air-conditioning water systems in supertall buildings: A pilot study.* Science and Technology for the Built Environment, 2018. **24**(4): p. 371-381.

42. Christensen, C., G. Barker, and S. Horowitz. *A sequential search technique for identifying optimal building designs on the path to zero net energy*. in *Proceedings of the Solar Conference*. 2004. American Solar Energy Society; American Institute of Architects.

43. Horowitz, S., et al., *Enhanced sequential search methodology for identifying cost-optimal building pathways*. 2008, National Renewable Energy Laboratory (NREL), Golden, CO.

44. Corporation, U. *http://unitil.com*. 2017; Available from: http://unitil.com.